^{14}N ENDOR of the OK1 centre in natural type Ib diamond

1989 J. Phys.: Condens. Matter 1 10549

(http://iopscience.iop.org/0953-8984/1/51/024)

J. Phys.: Condens. Matter 1 (1989) 10549–10561. Printed in the UK

^{14}N ENDOR of the OK1 centre in natural type Ib diamond

M E Newton and J M Baker
Clarendon Laboratory, Parks Road, Oxford OX1 3PU, UK

Received 9 August 1989, in final form 28 September 1989

Abstract. An ENDOR investigation has confirmed that the OK1 centre is a low-symmetry (σ_h) centre, incorporating a single nitrogen atom. The ^{14}N hyperfine and quadrupole coupling matrices have been determined by fitting the data to an exact solution of the energy matrix. Using this and other new experimental data we propose a model for this defect.

1. Introduction

Many different types of paramagnetic centre have been observed by magnetic resonance in diamond, but very few of them have been definitely characterised (Loubser and van Wyk 1978). The characterisation of most paramagnetic centres in other materials has been greatly facilitated by the presence of hyperfine structure, which gives an indication of the nuclei involved and the density of unpaired electrons on those nuclei. ENDOR measurements give more explicit information than ESR: (*a*) the value of g_N is obtained, so unambiguously identifying the nucleus involved, which facilitates clear interpretation of the hyperfine parameters in terms of densities of unpaired electrons on that nucleus; (*b*) the nuclear quadrupole interaction is measured, giving information about the electric field gradient at the nucleus due to all of the surrounding electrons, both paired and unpaired.

In diamond, the low abundance of magnetic isotopes of carbon (1.1% of ^{13}C), although it can lead to very narrow ESR lines, produces very weak hyperfine lines which are often unobservable. Hence there is often limited information about the distribution of the wavefunction of the unpaired electron over the neighbouring carbon atoms.

The easiest hyperfine structure to recognise in diamond has been that of nitrogen. As nitrogen comprises of nearly 100% ^{14}N, with $I = 1$, it leads to a clear three-line hyperfine structure; except in some centres where large quadrupole interaction leads to strong forbidden lines. As nitrogen is the only element for which nearly 100% of one isotope has $I = 1$, such a three-line structure is fairly certain identification.

Natural type Ib diamonds contain paramagnetic substitutional nitrogen (P1 centre), but some natural diamonds classified as type Ib also contain nitrogen in non-paramagnetic forms. Typical total nitrogen concentrations for natural type Ib diamonds range between 50–100 ppm. Natural type Ib diamonds contain large quantities of oxygen (600–11000 ppm Madiba *et al* (1988)). Almost all of the oxygen is incorporated in inclusions, with presumably only a small fraction actually incorporated in the diamond lattice. There are three predominant paramagnetic centres (P1, N3, OK1) involving a

0953-8984/89/5110549+13$02.50

single unpaired electron ($S = \frac{1}{2}$) and a single nitrogen atom ($I = 1$ for ^{14}N) in natural type Ib diamonds. They may all be described by the same spin Hamiltonian:

$$\mathcal{H} = \mu_B \boldsymbol{S} \cdot \mathbf{g} \cdot \boldsymbol{B} + \boldsymbol{S} \cdot \mathbf{A} \cdot \boldsymbol{I} + \boldsymbol{I} \cdot \mathbf{P} \cdot \boldsymbol{I} - \mu_N g_N \boldsymbol{I} \cdot \boldsymbol{B}. \tag{1}$$

The interaction matrices, whose form depends upon the symmetry of the site, are reading from left to right in equation (1): the electronic Zeeman interaction, the magnetic hyperfine interaction, the quadrupole interaction and the nuclear Zeeman interaction.

For a general site of low symmetry in diamond the T_d symmetry operations would generate 24 different orientations, but this number reduces as the site symmetry increases. Furthermore, there is sometimes a relatively low potential barrier between one site and another, so, at sufficiently high temperature, a centre may hop between different orientations, and if this occurs rapidly enough it leads to thermal averaging with a consequent simplification of the ESR spectrum.

The best characterised centre is the P1 (Smith *et al* 1959, Cook and Whiffen 1966, Barklie and Guven 1981). It comprises a substitutional nitrogen atom that forms four hybrid bonds with its neighbouring carbon atoms. The remaining unpaired nitrogen electron goes into an antibonding orbital directed along one of the four bonds. In this particular bond the electron pair is predominantly localised on the nitrogen atom, the unpaired electron is localised mainly on the carbon atom and the N–C separation is increased by about 10% (figure 1). This centre has C_{3v} symmetry about $\langle 111 \rangle$, with four possible sites. We used the well known ESR spectrum of this centre to deduce the orientation of the crystal planes in which our measurements were made. Above ~ 600 K motional averaging of the ESR spectrum starts to occur (Shul'man *et al* 1967), with the unpaired electron hopping between the four C–N bonds, at 1200 K the ESR spectrum is truly isotropic.

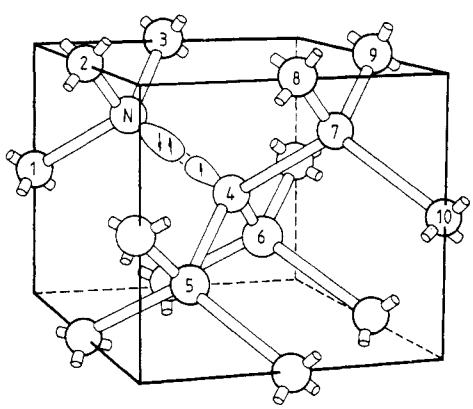

Figure 1. The P1 centre. The carbon atoms around the substitutional nitrogen atom are labelled 1 to 10, and are referred to in the text. The unique N–C bond is indicated with the electron pair predominately localised on the nitrogen, and the unpaired electron on the carbon.

The N3 centre was reported for the first time by Shcherbacova *et al* (1972). Van Wyk (1988) has shown that this centre with σ_h symmetry at room temperature, has a very small ^{14}N hyperfine interaction and a large quadrupole interaction: these

interactions have different principal axes. There are 12 symmetry related sites between which there is motional averaging at $\sim$ 550 °C, leaving at high temperature four sites with C_{3v} symmetry whose hyperfine and quadrupole interactions are now axially symmetric about $\langle 111 \rangle$. No definitive model has yet been proposed.

Reported ESR measurements (Klingsporn *et al* 1970) indicate that the OK1 centre has σ_h symmetry with $\{110\}$ as a principal plane, such that there are 12 possible defect sites. The g-matrix is slightly anisotropic, but close to 2.00. The anisotropic hyperfine interaction has previously been *incorrectly* fitted to the ESR data, because the quadrupole interaction has been ignored. Unlike that which occurs at the P1 and N3 centres, no motional averaging has been observed up to 600 °C. We report in this paper new measurements of ^{14}N ENDOR to determine the ^{14}N hyperfine and quadrupole interactions: using these with other information we propose a new model for the centre.

2. Experimental

2.1. ESR and ENDOR studies

The natural type Ib diamond studied was predominantly yellow/brown in colour, but optically very inhomogeneous. The sample was mounted on a perspex rod, and secured with vacuum grease or Araldite. The sample was mounted in one of two ways: either simply on one of the faces, or transferred (preserving orientation) from a goniometer, after x-ray orientation in a desired plane. This was inserted into the ENDOR cavity, which was attached to an Oxford Instruments ESR–9 flow cryostat, so that investigations could be made in the temperature range 3.7 K to 300 K, and the sample was rotated about a vertical axis in a horizontal magnetic field. The ENDOR cavity used was a TM_{110} cavity, operating at 9.313 GHz, similar in design to that of Möhl and de Boer (1985), but with iris coupling rather than a microwave loop, with modified microwave chokes and with a 115 kHz modulation coil inserted in the nodal plane of the microwave E-field. The RF coil construction followed that of Hurst *et al* (1982), the coil being embedded in heat-shrink tubing. This produced a free-standing durable coil, which can easily be changed and adjusted for critical coupling. The RF coil was driven by a Marconi 2022 signal generator, modulated at 87 Hz, and amplified by either a 40 W or 100 W ENI broad band radiofrequency amplifier. The ENDOR signal was detected using conventional phase sensitive detection (PSD) at 115 kHz of the first derivative ESR dispersion signal, followed by PSD at 87 Hz. For the OK1 centre the signal-to-noise ratio was poor, even at 4.2 K, so the final filtered PSD output was sent to a microcomputer for signal averaging.

To permit signal averaging over a period of 30 min the magnetic field was locked to a frequency modulated NMR proton probe (Robinson 1986), which had an inherent stability of a few parts in 10^6 over 30 min. This gave the magnetic field a long-term stability of much less than the ESR line width (0.05 mT). In all other respects the ENDOR spectrometer was of a conventional design.

To simplify the investigation specific ESR lines were chosen for ENDOR study. The angular variations of the ^{14}N ENDOR from the $M_I = +1$ ESR transitions for four defect sites were studied. Measurements were made in a (001) plane and a plane of known orientation close to a (110) plane, whose precise orientation was determined by the ESR of the P1 centre. This gave all the information required to fit the spin Hamiltonian

parameters. No measurements were made on the $M_I = 0$ ESR transitions because of the overlap with P1 and N3 centres.

2.2. Infrared absorption

Infrared (IR) absorption spectra were taken using a Perkin-Elmer 1710 IR Fourier transform spectrometer, at room temperature. In diamond, in the single-phonon region, there is absorption from three centres, the A and B centres and the P1 centre. The A defect consists of substitutional nitrogen pairs, and the B defect is a larger cluster of nitrogen atoms. The IR spectra in the one-phonon region of the diamond studied is shown in figure 2.

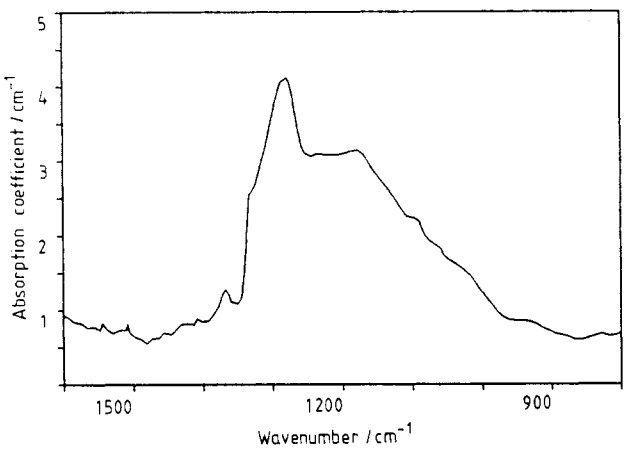

Figure 2. IR absorption spectrum of the type Ib diamond studied in the one-phonon region.

Spectra for pure A, B and P1 absorption are readily available in the diamond literature (Clark *et al* 1979): using these the spectra we can deconvolute the experimental spectra into its constituent A, B and P1 spectra, if we assume no other centre is responsible for absorption in this region. Using the coefficients determined by Woods *et al* (1988), we can calculate approximate nitrogen concentrations in the A, B and P1 defects, the results are summarised in table 1. The uncertainty in the magnitude of the measured absorptions is large, and there is much debate as to the values of the coefficients used to determine the nitrogen concentrations. It should also be remembered that the nitrogen concentrations possibly vary throughout the diamond. Hence the uncertainty in the A, B and P1 concentrations is large.

Table 1. Nitrogen concentrations calculated from IR absorption spectra in figure 2.

Impurity form	Wavenumber /cm^{-1}	Absorption /cm^{-1}	Nitrogen concentration/ppm
A	1282	2.4 ± 0.2	~ 40
B	1282	0.4 ± 0.2	~ 20
P1	1130	0.7 ± 0.2	~ 20

3. Results

3.1. ESR spectra

The relaxation times of the OK1 and P1 centres in the sample studied were such that ESR passage conditions could be observed. These are discussed, along with the information they reveal about spin–lattice relaxation times, in the Appendix. An angular variation of the ESR for the OK1 centre, in the plane close to a (110) plane, was measured at 4.2 K and could be fitted to the parameters determined from ENDOR; the anisotropy in the ESR is so small, that with an ESR line width of 0.05 mT it is not possible to resolve the ESR completely.

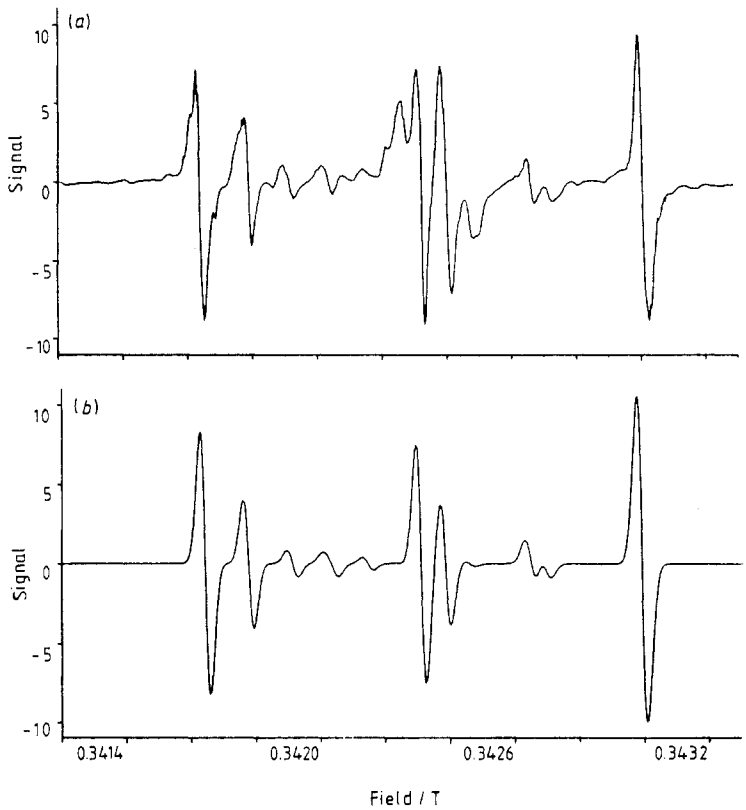

Figure 3. (*a*) Experimentally obtained ESR of the OK1 centre at 294 K with the magnetic field along [001] (approximately) and the microwave field along [110]. (*b*) Calculated ESR spectrum of the OK1 centre at 294 K with the magnetic field along [001] and the microwave field along [110].

Within the outer lines of the OK1 centre ESR there are a great many smaller lines, shown in figure 3(*a*), some of which are due to forbidden transitions between OK1 energy levels. The quadrupole interaction determined from the ENDOR investigation is significant when compared to the hyperfine interaction and gives rise to these forbidden transitions, which have an intensity of order $(P/A)^2$ relative to the main transitions. An exact solution of the energy matrix allows the intensities and positions of all ESR

transitions to be calculated. The calculated spectrum for the magnetic field along [001] and the microwave field along [110] is shown in figure 3(*b*). Comparison with figure 3(*a*) shows good agreement. The lines which have not been accounted for are due to other centres, including the P1 and N3.

An attempt was made to measure the unpaired electron density on the carbon atoms around the defect, through the ^{13}C hyperfine interaction. This isotope has a nuclear spin $I = \frac{1}{2}$, and is naturally 1.1% abundant. These transitions were detected, but owing to the low signal-to-noise ratio and the low symmetry of the centre, it was not possible to interpret the results unambiguously.

3.2. ENDOR spectra

At 4.2 K and below, the ESR could be saturated and ENDOR transitions observed. A typical ^{14}N ENDOR spectrum is shown in figure 4; the line width of about 120 kHz gives greatly improved resolution compared to the ESR. ENDOR transitions could in fact be observed at temperatures up to $\sim$ 10 K, but with a greatly reduced signal-to-noise ratio, compared to that at 4.2 K.

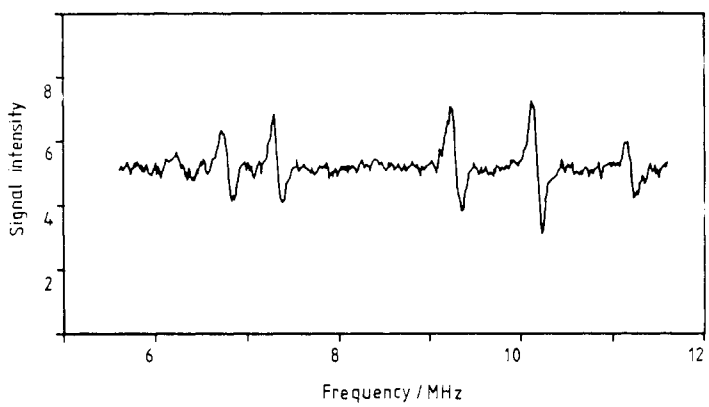

Figure 4. Typical ^{14}N ENDOR spectrum from $M_I = +1$ OK1 ESR transitions of four different sites at 3.7 K. Line width is about 120 kHz.

In figure 5, the ESR lines studied are drawn as full curves, and the ENDOR transitions are plotted as a function of orientation of magnetic field in the two planes studied in figure 6. The full curves represent a theoretical fit to the spin Hamiltonian, equation (1). All previous workers have ignored the ^{14}N quadrupole interaction when fitting the ESR by perturbation theory. This is not satisfactory, since the ^{14}N quadrupole interaction is sufficiently large to affect the positions of the ESR lines significantly. As perturbation theory is difficult to handle for this low symmetry, where principal axes of all the interactions are different, it proved better to solve the energy matrix exactly. A least squares fit to more than 150 data points produced the parameters in table 2, along with $g_N = 0.400 \pm 0.05$. The accepted value for ^{14}N is $g_N = 0.403$, proving beyond all doubt that the nucleus is ^{14}N. The fitting was performed subject to the constraint that {110} is a principal plane, as even with the greater precision of ENDOR there was no line doubling to suggest that this was not the case.

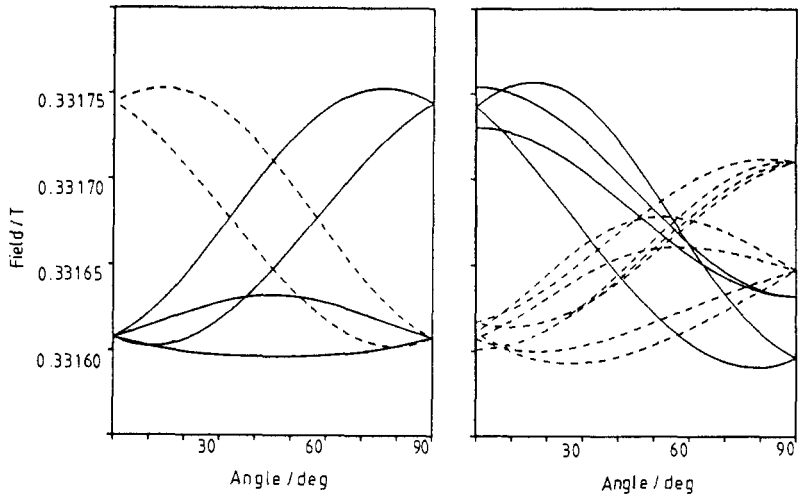

Figure 5. Angular variation of the $M_I = +1$ ESR in a ⟨001⟩ (left) plane and a plane of known orientation (right) which is close to a ⟨110⟩ plane. Orientation was determined from the P1 ESR. ENDOR transitions were measured using lines indicated by the full curves.

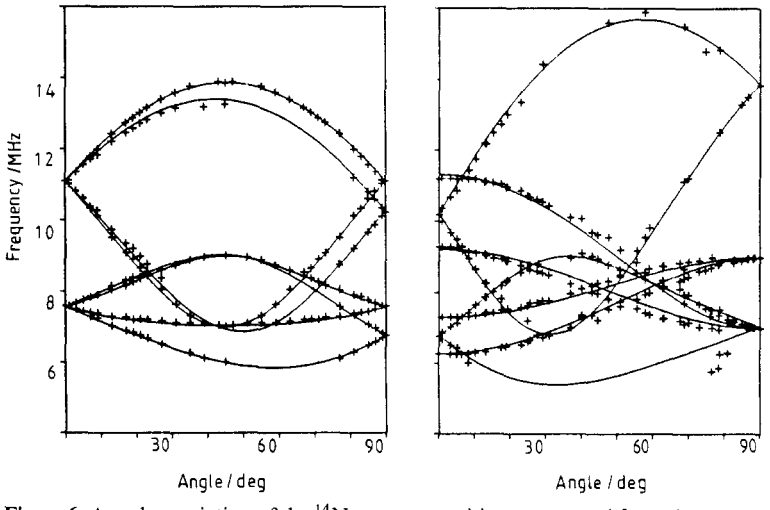

Figure 6. Angular variation of the ^{14}N ENDOR transitions, measured from the ESR transitions indicated in figure 5. The full curve represents the fit to the Hamiltonian, equation (1).

4. Discussion

4.1. *Information from* ENDOR

The ENDOR results have confirmed that {110} is a principal plane for the defect and that the nucleus giving rise to the hyperfine splitting is ^{14}N. The hyperfine matrix for the OK1 defect is compared with that for the N3 and P1 defects in table 3.

The unpaired electron spin densities given in table 3 are determined to first order by assuming that the electron wavefunction ψ_N on ^{14}N is a linear combination of

Table 2. New hyperfine and quadrupole parameters for the OK1 centre. A_1 and P_1 correspond to a $\langle 1\bar{1}0\rangle$ direction, and A_2 and P_2 make angles of 25.0° and 36.1° (±0.3°) respectively with $\langle 110\rangle$.

Hyperfine parameters ±0.02 MHz	Quadrupole parameters ±0.02 MHz
$A_1 = 15.48$ MHz	$P_1 = +1.31$ MHz
$A_2 = 21.66$ MHz	$P_2 = -2.67$ MHz
$A_3 = 15.19$ MHz	$P_3 = +1.36$ MHz

Table 3. The hyperfine, quadrupole parameters, p/s ratio of the unpaired electron orbital, and its density on ^{14}N for the P1, OK1 and N3 centres in type Ib diamond. A_1 and P_1 correspond to a $\langle 1\bar{1}0\rangle$ direction, and A_2 and P_2 make angles of θ° and ϕ° respectively with $\langle 110\rangle$. Angles are measured from $\langle 110\rangle$ towards $\langle 111\rangle$. P1 data from Cook and Whiffen (1966) and N3 data from van Wyk (1988).

Defect	Hyperfine matrix/MHz				Quadrupole matrix/MHz				p/s	% on
name	A_1	A_2	A_3	θ/deg	P_1	P_2	P_3	ϕ/deg	ratio	^{14}N
P1	81.34	113.98	81.34	35.3	+1.32	−2.65	+1.32	35.3	3.85	25
OK1	15.48	21.66	15.19	25.0	+1.31	−2.67	+1.36	36.1	3.93	5
N3	3.12	4.28	3.12	26.0	+1.88	−3.77	+1.88	34.5	3.74	1

nitrogen ψ_{2s} and ψ_{2p} atomic orbitals.

$$\psi_N = c_s\psi_{2s} + c_p\psi_{2p} \tag{2}$$

The coefficients c_s and c_p are determined, in the usual fashion from the hyperfine matrix (Smith *et al* 1959). The ratio $p/s = c_p^2/c_s^2$ is the ratio of electron densities in ψ_{2s} and ψ_{2p} states, and is listed in table 3. The small departure from axial symmetry for the OK1 centre is ignored in the determination of the p/s ratio, it is probably due to spin polarisation. The total unpaired electron density on ^{14}N is $(c_p^2+c_s^2)$ and in the OK1 and N3 centres is very small, much less than in the P1 centre. This small localisation on the nitrogen is probably because all the nitrogen orbitals contain electron pairs, resulting in little mixing of the unpaired electron on the nitrogen. However, the p/s ratios for the unpaired electron orbital in the P1 and OK1 defects are almost identical (table 3), indicating that this orbital is the same in both defects. The unpaired electron orbital must be orthogonal to the bonding orbitals surrounding the nitrogen atom. Therefore the hyperfine measurements imply that the electronic orbitals around the nitrogen atom must be identical in both the OK1 and P1 defects, but with lower unpaired electron density on the nitrogen atom for OK1. This analogy between systems is supported by the measurement of the ^{14}N quadrupole interaction.

The quadrupole interactions of the three defects are listed in table 3. The significant new information about the OK1 centre given by our measurements is that the ^{14}N quadrupole interaction is to within experimental error identical with that of the P1 centre. This means that the electric field gradients (EFG) at both nitrogen sites are identical. To a good approximation the EFG arises only from electron orbitals which depend on the anisotropic nitrogen atomic orbitals (ψ_{2p}); since the EFG matrix elements have a $\langle r^{-3}\rangle$ dependence (r is the distance from the nitrogen nucleus). In figure 1 the P1 centre is shown with carbon atoms labelled numerically.

For P1, Every and Schonland (1965) attempted to calculate the EFG at the nitrogen nucleus. Their calculation assumes that the paired electrons in the three equivalent N–C bonding orbitals (carbon atoms 1, 2 and 3) are equally shared between the nitrogen and the carbon. This is not likely to be the case because of the displacement of the nitrogen atom towards the plane containing these three atoms. Every and Schonland's calculation shows that the major part of the quadrupole interaction is produced by paired electrons in the three equivalent N–C bonding orbitals and in the unique N–C bond, where most of the electron pair is located on the nitrogen atom because of the greatly increased N–C distance. We believe that a calculation with the distortion of the three N–C basal orbitals included would increase the dominance of the paired electron contribution to the EFG. Hence we believe that the unpaired electron does not contribute significantly to the EFG in either P1 or OK1 defects. The equivalence of the quadrupole interactions suggests that the configuration of paired electrons around the nitrogen is the same in both defects, though the hyperfine interaction indicates lower unpaired electron density on the nitrogen in OK1.

4.2. *Possible models for the OK1 defect*

Two models have been previously proposed for the OK1 centre, (i) McNeil and Symons (1977) proposed that the unpaired electron was principally confined to an oxygen atom and postulated an atomic arrangement N–C–O for the defect, since this is very common in nature, and Shcherbacova *et al* (1972) proposed that the OK1 centre is a substitutional nitrogen next to a lattice vacancy, [Nitrogen + Vacancy]°.

Because of the equality of the quadrupole interactions we regard OK1 as a perturbed P1 centre. To produce σ_h symmetry relative to the {110} plane containing atoms 1,4,7,10 (figure 1) the perturbation must occur in that plane. This type of distortion would be consistent with the [Nitrogen + Vacancy]° model, involving a vacancy at site 4, the analogue of the Si-G8 centre ([Phosphorus + Vacancy]°) in silicon (Watkins and Corbett 1964), as a bonding orbital is formed between atoms 5 and 6, and the unpaired electron is located primarily upon atom 7. However, one would expect some increase in the quadrupole interaction; and other properties of OK1 which are difficult to reconcile with the model are (*a*) lack of thermal averaging at high temperatures, (*b*) it is not created by electron irradiation like the Si-G8 centre, and (*c*) when the sample is heated in the dark enabling the OK1 to capture an electron, it does not produce a W15 centre which has been shown to be a substitutional ^{14}N plus a vacancy which has captured an electron (Loubser and van Wyk 1977). Any model involving a vacancy is unlikely, as the OK1 centre is not created by electron irradiation which generates vacancies.

A second substitutional impurity in the plane containing atoms 1,4,7,10 would produce the required symmetry, though site 10 is probably too far away to produce the marked change in density of unpaired electron on the nitrogen atom; so the likely sites for an impurity are 7 and 4. As no hyperfine structure is observed, any impurity involved is likely to be an atom with very low abundance of isotopes with nuclear spin. Of the impurities that occur in diamond, this suggests: O, S, Ca or Ni, of which Ca is unlikely because OK1 can occur up to 100 ppm, which is much greater than observed Ca concentrations. Ni seems unlikely as one should be able both to observe interaction between its unfilled 3d shell and the unpaired electron, and to produce by irradiation Ni^+ or Ni^- whose ESR would be observable. S is unlikely, as in diamonds containing both OK1 and S, the S gives rise to the W31 centre (van Wyk and Loubser 1986). This leaves O as a possible constituent of the OK1.

Recent work (Madiba *et al* 1988) has shown that the number of OK1 centres is correlated with the oxygen content of the sample, although the number of P1 centres is not. This supports the proposal of McNeil and Symmons (1977) that oxygen is incorporated in the defect. Although the majority of the oxygen is known to be in the form of inclusions, it is possible that a small fraction of it is incorporated as atoms in the lattice. There is however no evidence about how the oxygen atom is incorporated into the diamond. The relative total energy of substitutional and interstitial impurities in silicon has recently been investigated (Weinert *et al* 1988). Oxygen and carbon impurities on interstitial sites are energetically favoured to substitutional sites in silicon because they have a smaller covalent radius than the host. However, sulphur, which has similar covalent radius to silicon, has lower energy in a substitutional site. Since carbon and oxygen have similar covalent radii, we expect that an oxygen atom on a substitutional site would be favoured in diamond. There appear to be only two substitutional sites for the oxygen atom that would perturb P1 sufficiently: site 4 and site 7, figure 1.

An oxygen atom at site 4 would distort to form a C–O–C bond between atoms 5 and 6, leaving the unpaired electron on site 7. This unpaired electron would form a weak bonding orbital with the nitrogen, which could account for the observed hyperfine interaction. However, one might expect thermally excited hopping of the C–O–C bond between sites 5, 6 and 7 at high temperatures, which is not observed for OK1. In addition, one would expect the quadrupole interaction to be increased somewhat by replacing the carbon atom at site 4.

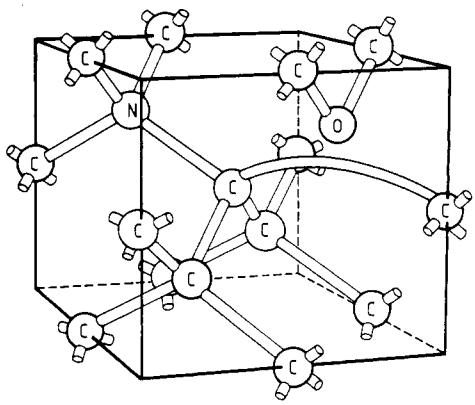

Figure 7. New model for OK1 centre based on experimental evidence presented in this paper. This centre is the analogue of the Si-B1 centre in silicon, where the additional electron has been donated by the nearby substitutional nitrogen atom.

An oxygen atom at site 7 would be the analog of the Si-B1 centre in a silicon (Watkins and Corbett 1961a) where the additional electron had been donated by a nearby substitutional impurity. The oxygen atom would form a C–O–C bond between atoms 8 and 9, and the dangling orbitals on 4 and 10 would form a bonding orbital. The unpaired electron goes into an antibonding orbital between 4 and 10, as that has a lower energy than an antibonding orbital between 4 and the nitrogen, and this would have some overlap with the wavefunction on the nitrogen giving the observed hyperfine structure. As the four ligands of the nitrogen are the same in this model as in P1, except for possible small displacement of atom 4, one expects the same

quadrupole interaction; and as exchange in position of oxygen and carbon atoms would be necessary to change from one σ_h site to another, one would not expect thermally activated averaging. Hence this seems the most likely model for the OK1 centre. This model for the OK1 centre is shown in figure 7.

We must point out that this model is very different from that proposed by McNeil and Symons (1977). They proposed that the unpaired electron was principally confined to the oxygen atom: in the model proposed here the unpaired electron is principally confined to an extended C–C bond.

Unfortunately, it would be extremely difficult to prove that oxygen is involved in this site even if it were possible to have diamonds enriched with ^{17}O, because the oxygen lies at the antinode of the antibonding orbital and so should give a very small hyperfine structure. Watkins and Corbett (1961a) could not identify oxygen as a constituent of the Si-B1 centre from ESR, even though they had samples doped with ^{17}O. The configuration of oxygen in the Si-B1 defect was established by infrared absorption (Watkins and Corbett 1961b).

It is interesting to note that no centre similar to the OK1 centre has been identified in silicon. However, Watkins and Corbett (1964) do mention a weak ESR spectrum which displayed phosphorus hyperfine structure. This centre could be tentatively associated with a phosphorus atom paired off with another defect, possibly an oxygen atom. Could this be a phosphorus atom near an A centre, the analogue of the OK1 centre in diamond?

Acknowledgments

The authors are indebted to Professor J H N Loubser and Dr J A van Wyk for encouragement, guidance and many helpful discussions. Acknowledgement is made to De Beers Industrial Diamond Division for samples and financial support.

Appendix

A comprehensive review of passage effects has been undertaken by Weger (1960). In our sample, studied between 3.7 K and 300 K, the spin–lattice relaxation times (T_{1e}) of both centres were such that the ESR signals could be detected under adiabatic or non-adiabatic rapid passage conditions, called ARP and NARP respectively. At and below room temperature the OK1 and P1 ESR could be saturated with the available microwave power (< 150 mW); saturation is essential for both ARP and NARP. ARP produces ESR signals with unusual shaped absorption and dispersion signals, which can be used to identify the condition, figure 8.

The ARP signal is out of phase with that of an unsaturated ESR signal, the phase shift depending on T_{1e} and the modulation frequency. The critical experimental parameters are the microwave magnetic field, the field modulation frequency (115 kHz) and amplitude, the ESR line width, the rate of field sweep and of course T_{1e}, which is temperature dependent. With saturation, low modulation amplitude, and a rapid field sweep, ARP can be observed. From ARP with a small burnout of magnetisation, the range of T_{1e} can be estimated. At 294 K for both centres 0.1 ms < T_{1e} < 10 ms, and saturation indicates that T_{1e} for the OK1 centre is much smaller than that of the P1 centre. The values determined in other diamonds (Barklie and Guven 1981,

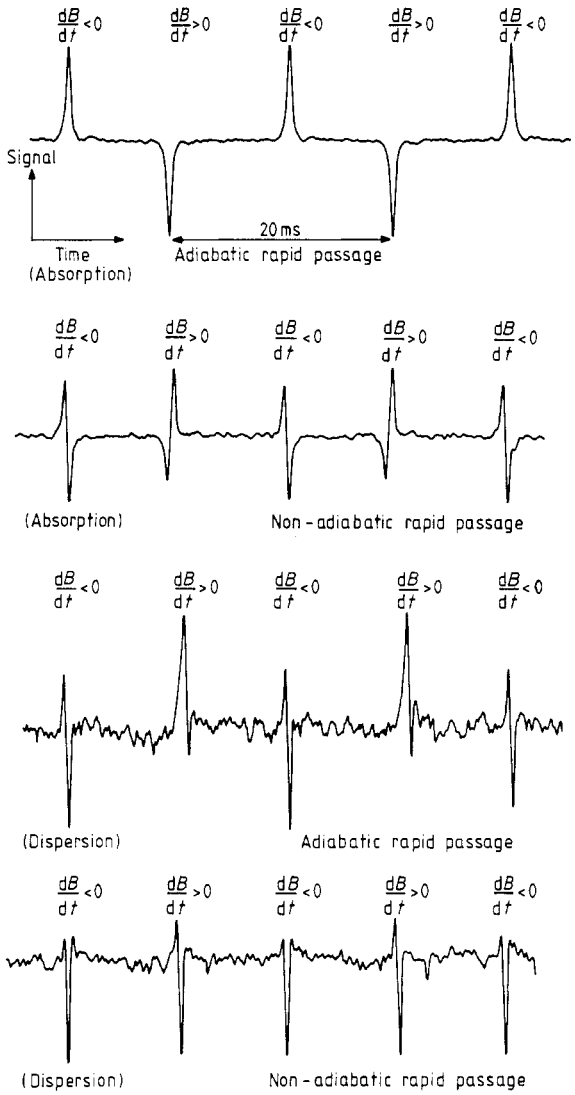

Figure 8. Absorption and dispersion spectra recorded under ARP and NARP for the P1 centre in the type Ib diamond studied. Magnetic field swept through resonance with 50 Hz sinusoidal oscillator, therefore spectra repeat every 20 ms.

Campbell 1987) for the P1 centre lie in this range. ARP of the P1 ESR under conditions of strong saturation produced a much greater signal-to-noise ratio than conventional ESR. Violating the adiabatic condition, by either reducing the microwave magnetic field strength or increasing the modulation amplitude, permits the observation of NARP. The line shapes for NARP are the same as for an unsaturated signal.

References

Barklie R C and Guven J 1981 *J. Phys. C: Solid State Phys.* **14** 3621
Campbell I D 1987 *J. Mag. Res.* **74** 155

Cook R J and Whiffen D H 1966 *Proc. R. Soc.* A **295** 99
Every A G and Shonland D S 1965 *Solid State Commun.* **3** 205
Clark C D, Mitchell E W J and Parsons B J 1979 *The Properties of Diamond* ed J E Field (New York: Academic) p 21
Hurst G, Kraft K, Schultz R and Kreilick R 1982 *J. Mag. Res.* **49** 159
Klingsporn P E, Bell M D and Levio J 1970 *J. Appl. Phys.* **41** 2977
Loubser J H N and van Wyk J A 1977 *Diamond Research 1977* (Ascot: De Beers Industrial Diamond Division) p 11
—— 1978 *Rep. Prog. Phys.* **41** 1210
Madiba C P P, Sellschop J P F, van Wyk J A and Annergarn H J 1988 *Diamond Conference, Cambridge*
McNeil D A C and Symons M C R 1977 *J. Phys. Chem. Solids* **38** 397
Möhl W and de Boer E 1985 *J. Phys. E: Sci. Instrum.* **18** 479
Robinson F N H 1986 *J. Phys. E: Sci. Instrum.* **20** 502
Shcherbacova M Ya, Sobolev E V and Nadolinnyi V A 1972 *Sov. Phys.–Dokl.* **17** 513
Shul'man L A, Zaitskii I M and Podzyarei G A 1967 *Sov. Phys.–Solid State* **8** 1842
Smith W V, Sorokin P P, Gelles I L and Lasher G J 1959 *Phys. Rev.* **115** 1546
van Wyk J A 1988 *Diamond Conference, Cambridge*
van Wyk J A and Loubser J H N 1986 *Defects in Semiconductors, Mat. Sci. Forum* **10–12** 923
Watkins G D and Corbett J W 1961a *Phys. Rev.* **121** A1001
—— 1961b *Phys. Rev.* **121** A1015
—— 1964 *Phys. Rev.* **134** A1359
Weger M 1960 *Bell Syst. Tech. J.* 1013
Weinert C M, Beeler F and Scheffer M 1988 *J. Phys. C: Solid State Phys.* **21** 841
Woods G S, Collins A T and Harris J W 1988 *Diamond Conference, Cambridge*